SCIENTIFIC REPORTS

OPEN

SUBJECT AREAS:
SOLAR CELLS
ELECTRONIC MATERIALS

Received
31 March 2014

Accepted
13 June 2014

Published
4 July 2014

Correspondence and requests for materials should be addressed to R.G. (gaorui_2013@tsinghua.org.cn) or L.D.W. (chldwang@mail.tsinghua.edu.cn)

# Multifunctional Interface Modification of Energy Relay Dye in Quasi-solid Dye-sensitized Solar Cells

Rui Gao[1], Yixiu Cui[1], Xiaojiang Liu[1] & Liduo Wang[2]

[1]Institute of Electronic Engineering, China Academy of Engineering Physics, Mianyang 621900, Sichuan, China, [2]Key Lab of Organic Optoelectronics & Molecular Engineering of Ministry of Education, Department of Chemistry, Tsinghua University, Beijing 100084, China.

**In this paper, 4-(dicyanomethylene)-2-t-butyl-6(1,1,7,7-tetramethyljulolidyl-9-enyl)-4H-pyran (DCJTB) has been used in interface modification of dye-sensitized solar cells (DSCs) with combined effects of retarding charge recombination and Förster resonant energy transfer (FRET). DCJTB interface modification significantly improved photovoltaic performance of DSCs. I–V curves shows the conversion efficiency increases from 4.27% to 5.64% with DCJTB coating. The application of DCJTB with combined effects is beneficial to explore more novel multi-functional interface modification materials to improve the performance of DSCs.**

Since 1991, dye-sensitized solar cells (DSCs) have attracted much attention worldwide due to its lower production cost and easier fabrication[1]. Much work has been done on dye molecules[2,3], photoanode[4], electrolyte[5] and counter electrode[6] to improve the photovoltaic performance of DSCs. Now the highest conversion efficiency over 12% has been achieved[7].

In DSCs, the interface between sensitized $TiO_2$ and electrolyte plays a vital role in the photovoltaic performance[8,9] as several important reactions or processes occur here, such as electron injection, charge transfer, charge recombination and dye regeneration. Interface modification and additives in electrolyte have been demonstrated effective ways to enhance the conversion efficiency and improve the stability of DSCs[10–15]. Earlier studies focused mainly on control and modification of metal oxide[14] or carboxylate[13]. Such work improved the performance of DSCs mainly through retarding the charge recombination. Recently, a new kind of interface modification material has been developed to improve the performance of DSCs, which acts as energy relay dye (ERD) that could enhance the photoresponse through Förster resonant energy transfer (FRET) effect, in addition to retarding surface charge recombination[16].

FRET involves dipole–dipole coupling of ERD and acceptor through an electric field, which has been applied in DSCs and polymer solar cells to enhance their photoresponse and obtained excellent results[17]. FRET also occurs between quantum dots and organic dyes, which improves the photo capture[18–20]. Excitation of ERD could be non-radiative transfer to the acceptor dye through the electric field as the emission spectrum of the ERDs overlaps with the absorption spectrum of acceptors[21–23]. FRET efficiency between ERDs and acceptors mostly depended on the Förster radius ($R_0$). ERDs applied in DSCs were commonly dispersed in the liquid electrolyte[24]. In such a configuration, many ERD molecules cannot transfer energy effectively as they were far away from the acceptor dyes attached on the $TiO_2$ surface. Furthermore, the solvent could cause the ERDs elicitation quenching. Assembling ERDs on the interface would avoid such disadvantages as they are concentrated at the interface of sensitized photoanode and electrolyte[25–26]. The distance between ERDs and acceptors is short and the contact of ERD and solvent in electrolyte is minimized or avoided as well.

In this paper, 4-(dicyanomethylene)-2-t-butyl-6(1,1,7,7-tetramethyljulolidyl-9-enyl)-4H-pyran (DCJTB) has been applied as ERD in DSCs, which was widely used in organic light emitting diode (OLED)[27], but has never been explored in DSCs. N3 dye was used as the acceptors. Absorption peak of N3 well overlapped with the emission peak of DCJTB, assuring the effective FRET between them. Using DCJTB in the interface modification, photovoltaic performance of DSCs has been improved due to DCJTB's combining effects of FRET and retarding charge recombination.

## Experimental

The $TiO_2$ colloid was prepared with a hydrothermal method, which has been well documented in the previous report[28]. To prepare porous $TiO_2$ film, transparent conductive FTO glass (12Ω square$^{-1}$) was thoroughly cleaned and a thin compact $TiO_2$ film (about 8 nm in thickness) was subsequently deposited on the FTO by dip coating in order to improve ohmic contact and adhesion between the following porous $TiO_2$ layer and the conductive FTO glass. The doctor blade technique was then adopted to prepare the porous $TiO_2$ layer, the thickness of the porous layer being controlled by an adhesive tape. Afterwards, the film was thermo-treated at 450°*C* for 30 *min*. When cooled to 110°*C*, the $TiO_2$ electrode was sensitized by immersion in 0.3 *mmol* $L^{-1}$ N3 absolute ethanol solution for 12 h and cleaning with absolute ethanol. Coating of DCJTB was performed as follows: the saturated ethanol solution of DCJTB was dipping on the sensitized $TiO_2$ film, then dried in air for 30 min to make it concentrated on the surface of $TiO_2$ film. The N3 sensitizer was commercially available. DCJTB has been synthesized as in the Ref. 29.

The preparation procedure for the polymer gel electrolytes includes two steps. First, liquid electrolyte was prepared. Second, poly (ethylene oxide) (PEO) was slowly added into the liquid electrolyte and heated under strong stirring until the polymer gel electrolyte became homogeneous. The composition of the liquid electrolyte is as follows: 0.1 *mol* $L^{-1}$ LiI, 0.1 *mol* $L^{-1}$ $I_2$, 0.6 *mol*$L^{-1}$ 1,2-dimethyl-3-propyl imidazolium iodide (DMPII), and 0.45 *mol*$L^{-1}$ N-methyl-benzimidazole (NMBI). The solvent was 3-methoxypropionitrile (MePN)[30]; the weight ratios (versus liquid electrolyte) for the PEO in the electrolyte was 10.0%.

A chemically platinized conductive glass was used as the counter electrode. When assembling the DSCs, the polymer gel electrolyte was sandwiched by a sensitized $TiO_2$ electrode and a counter electrode with two clips; the space between the two electrodes was controlled by an adhesive tape with a thickness of 30 *μm*. Finally, the DSCs were baked at 80°*C* to ensure the polymer could penetrate into the nanoporous electrode.

The UV-Vis reflectance absorption spectra were measured with a Hitachi U-3010 spectroscope. The Photocurrent-voltage (I–V), EIS, IMVS and IMPS were investigated by ZAHNER CIMPS electrochemical workstation. The incident photon-to-current conversion efficiency (IPCE) was measured by using a lab-made IPCE setup in Professor Meng's laboratory in Institute of Physics, Chinese Academy of Sciences.

## Results and discussion

Figure 1 shows the UV-vis absorption spectra of N3, DCJTB and emission spectrum of DCJTB in solutions and adsorbed on $TiO_2$ film. One can see from Figure 1(a) that the emission peak of DCJTB differed from the adsorption peak of N3 in the solution, which are 620 nm and 530 nm, respectively. However, Figure 1 (b) reveals that the emission peak of DCJTB shifts to 560 nm when assembled on the $TiO_2$ surface, which is the same situation in the DSCs devices as using the dip-coating method to concentrate ERD at the interface of photoanode and electrolyte. Such a good overlap would promote effective FRET between them. The shift of emission peak could be attributed to the aggregation or close assembly of the DCJTB molecules on the surface of $TiO_2$ film. Besides, the emission peak of DCJTB on the $TiO_2$ surface also becomes much narrower, which is due to the aggregation-induced emission effect[31].

The Förster radius ($R_0$) is the distance that FRET is 50% probable between ERD and acceptors. It could be calculated using equation (1)[32].

$$R_0^6 = \frac{9000 * \ln(10)\kappa^2 Q_D}{128 * \pi^5 n^4 N_A} \int F_D(\lambda)\varepsilon_A(\lambda)\lambda^4 d\lambda \qquad (1)$$

Where $n$ is the index of refraction of the host medium, $\kappa^2$ is the orientation factor (2/3 for random orientation, which could be used

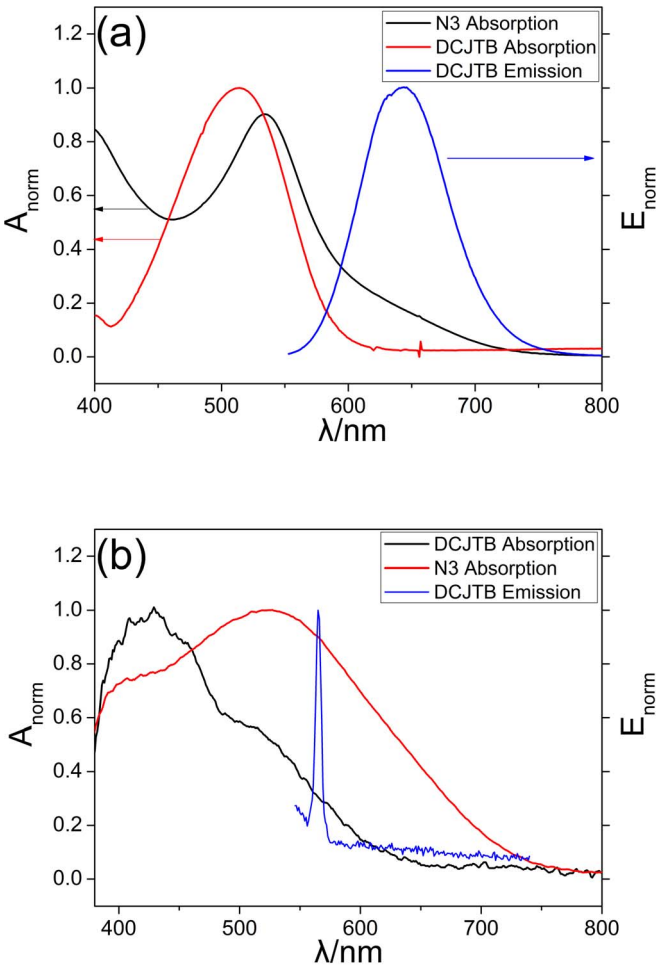


**Figure 1 | UV-vis absorption spectra of N3, DCJTB and emission spectrum of DCJTB (a) in solutions and (b) on $TiO_2$ film.**

in DSCs system), $N_A$ is Avogadro's number, $Q_D$ is photoluminescence efficiency of ERDs, and *FD* is the emission profile of the donor. $\varepsilon(\lambda)$ is the molar absorption coefficient at certain wavelength[32]. For the DCJTB/N3 system, it could be calculated the $R_0$ is 5.2 nm.

The rate of FRET between isolated chromophores has been known as point to point transfer. It is given by equation[32]:

$$k_{FRET} = k_0 * \frac{R_0^6}{r^6} \qquad (2)$$

where $r$ is the separation distance between ERDs and acceptors, $k_o$ is the Boltzmann constant and $R_o$ is the Förster radius calculated from Eq 1. Equation (2) reveals that with a given $R_o$, r is the most important factor that determines the efficiency of FRET[32].

As shown in Figure 2 (a), adding N3 into the DCJTB solution, the emission intensity decreased to about 47.8% of the initial value. It indicates that the excitation of DCJTB has been partly transferred to N3. However, the efficiency of FRET between DCJTB and N3 is not high enough due to the much larger distance between N3 molecules and DCJTB than $R_0$ calculated from equation (1) in the solution system. Besides, emission peak of DCJTB and absorption peak of N3 does not overlap so well, as shown in Figure 1(a). Figure 2 (b) reveals that the emission of DCJTB almost disappeared totally when assembled on the surface of $TiO_2$ film, suggesting much higher energy transfer efficiency than that in the solution. It could be explained that on $TiO_2$ surface the distance of DCJTB and N3 has been shortened as they both are assembled on the same surface. As a result, the FRET efficiency has been enhanced significantly. Thus, the dip-coating method, which concentrates ERD and acceptors on the

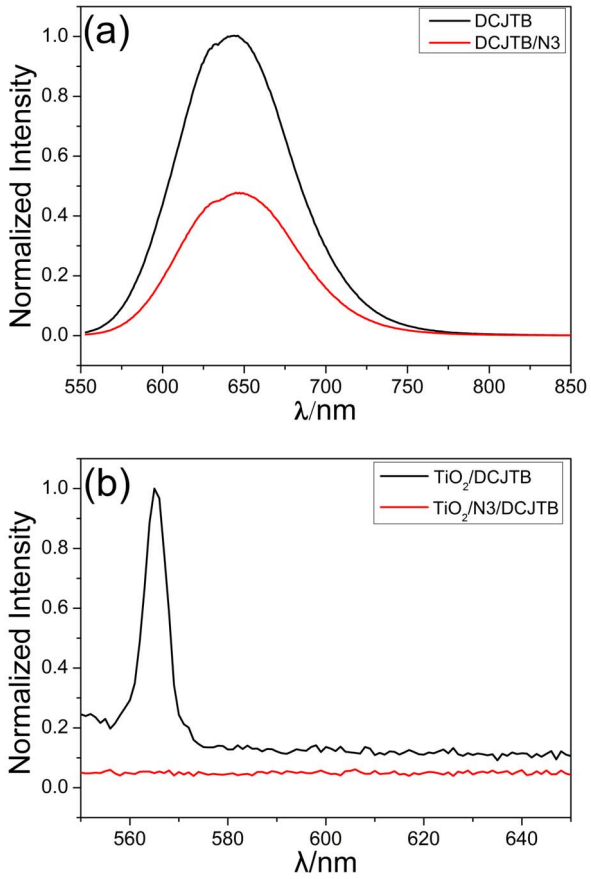


**Figure 2 | (a) fluorescence emission spectra in solution (b) fluorescence emission spectra on $TiO_2$ film of DCJTB and DCJTB/N3.**

surface of $TiO_2$ photoanode, has been used to obtain a better FRET efficiency in DSCs. Figure 3 shows the schematic drawing of FRET in DSCs using DCJTB as ERD and N3 as acceptors. The excitation of DCJTB transfers to N3 through FRET, and subsequently the electrons injects to the conductive band of $TiO_2$, which could increase the photoresponse and photocurrent of DSCs.

As DCJTB molecules are concentrated on the surface of sensitized $TiO_2$, shortening the distance between ERD and acceptors. Thus the FRET could occur more effectively than that with dispersing ERDs in the electrolyte reported in previous studies[33–34]. Figure 4 (a) shows that with DCJTB coating on the sensitized $TiO_2$ film, IPCE of DSCs increased clearly in the range of 380–500 nm. This increase is attributable to the effective FRET from DCJTB to N3. And then the

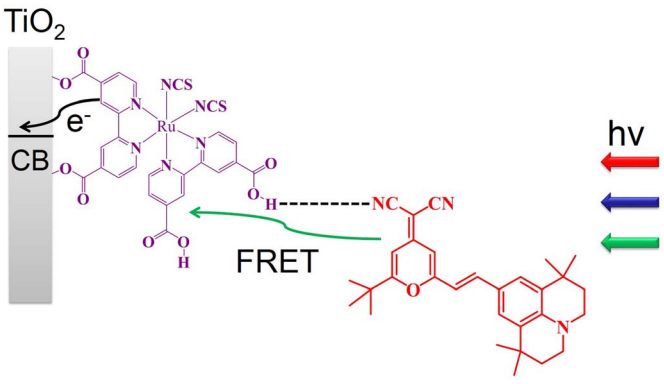


**Figure 3 | Diagrammatic drawing of FRET in DSCs using DCJTB as ERD.**

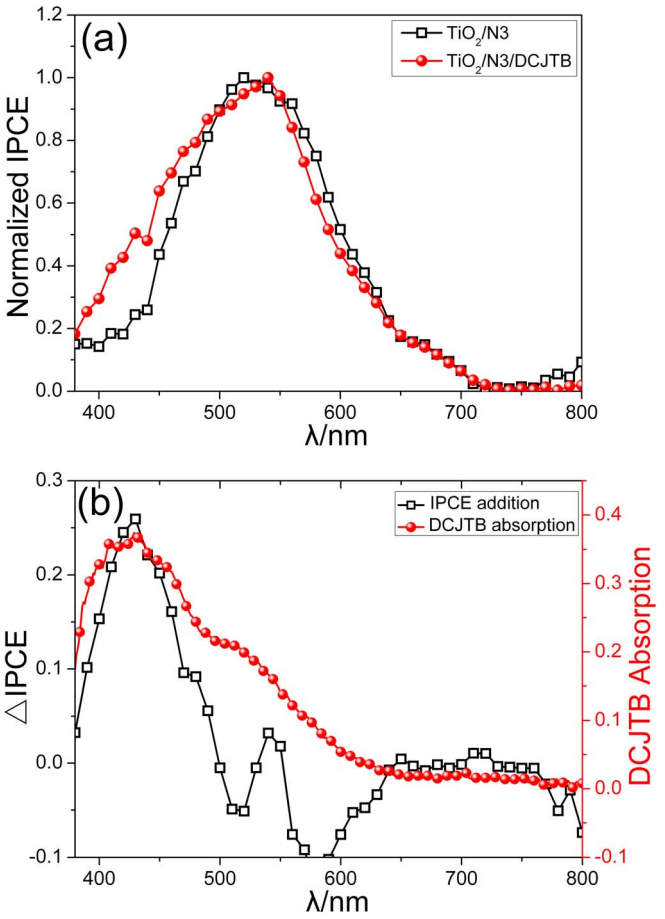


**Figure 4 | (a) IPCE spectra of DSCs with and without DCJTB coating (b) comparison between additional IPCE and absorption of DCJTB.**

additional electrons of N3 inject into the conductive band of $TiO_2$, which could increase the photocurrent of DSCs. As revealed in Figure 4 (b), additional IPCE with DCJTB coating in the range of 380–500 nm overlaps well with the absorption peak of DCJTB. This result further indicates that FRET from DCJTB to N3 in DSCs system effectively occurred on the sensitized $TiO_2$ film.

The results of IPCE show that the FRET between DCJTB and N3 increased photoresponse of DSCs devices, which could enhance the photocurrent. To investigate the effects of FRET on the DSCs' photovoltaic performance, we tested the I–V curves of DSCs without and with DCJTB coating. As shown in Figure 5 (a) and Table 1, the $J_{sc}$ increases from 12.96 without DCJTB coating to 16.63 mA/cm$^2$ with DCJTB coating, i.e., 28.3% enhancement in short-circuit current density. It accords with the increase of IPCE shown in Figure 4. The power conversion efficiency of DSCs with DCJTB coating was found to be increased to 5.64% from 4.27%, or relative enhancement of 32%. In the early studies reported in literature[33–34], the increased power conversion efficiency was mainly due to the increased $J_{sc}$ caused by FRET between ERD and acceptors, while $V_{oc}$ remained unchanged or even decreased. However, the present study revealed an appreciable increase in open circuit voltage, $V_{oc}$, from 0.65 V to 0.69 V with DCJTB coating as shown Figure 5(a) and Table 1. Figure 5 (b) also showed that the dark current density appreciably decreased with DCJTB coating, indicating that the charge recombination at the electrode and electrolyte interface in DSCs was hindered by the insertion of DCJTB coating, as a barrier layer which retards the charge recombination in DSCs as its higher LUMO energy level than that of N3 as shown in Figure 6[35–36]. To further explore the effect of retarding charge recombination in DSCs with DCJTB coating, EIS has been tested.

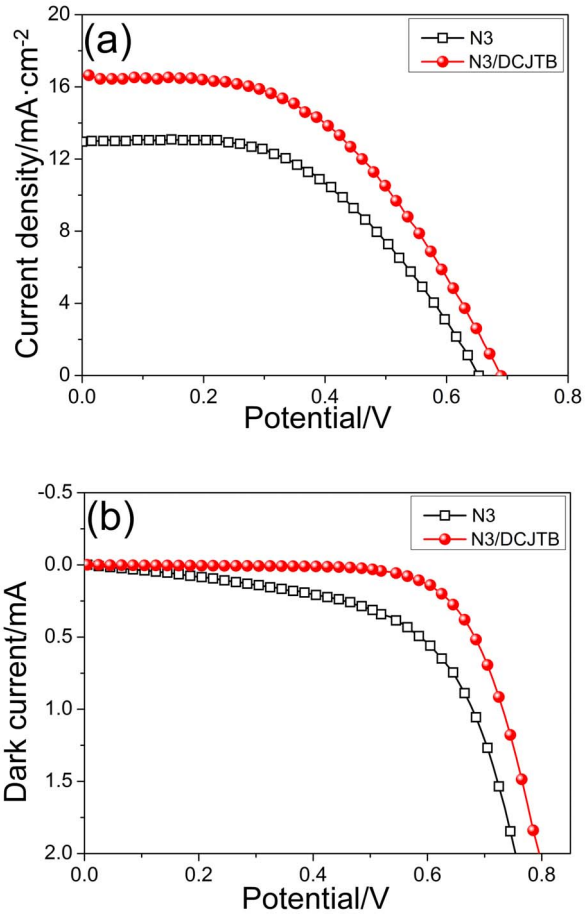


**Figure 5 | (a) I–V curves under illumination of 100 mW cm$^{-2}$ (b) Dark current curves of DSCs with and without DCJTB coating.**

As shown in the equivalent circuit inserted in Figure 7 (a), the impedance associates with the charge transfer process occurring at Pt counter electrode/electrolyte interface is determined in the frequency range of $10^5$–$10^3$ Hz, which is characterized by the charge transfer resistance ($R_1$) and the capacitance ($CPE_1$). In the middle frequency range of $10^3$–$10^0$ Hz, the impedance representing the charge recombination process at the $TiO_2$/dye/electrolyte interface is described by $R_2$ and the $CPE_2$. In the low frequency range or 0.1–10 Hz, the Warburg diffusion impedance ($Z_w$) within the electrolyte is estimated. $Z_w$ accounts for a finite length Warburg diffusion while CPE represents the constant phase element[37–40].

As DCJTB has been concentrated at the interface of sensitized $TiO_2$ and electrolyte, we focused on its effects on the charge recombination at such interface ($R_2$). As shown in Figure 7 (a), the charge recombination resistance increases with DCJTB coating. Thus the back reaction in DSCs has been decreased. Such result also accords with the higher $V_{oc}$ and lower dark current shown in Figure 5. Figure 7 (b) shows the Bode pots of DSCs based on photoanode without and with DCJTB coating. The three peaks in the phase of the spectrum are associated with three transient processes in the DSC. The middle-frequency peak (in the 10–100 Hz range) is determined by the lifetime of the electrons in $TiO_2$, which is also the charge recombination time in dark condition. It is shown as follow equation[41]

$$\tau_r = \frac{1}{2\pi f_{\min}} \quad (3)$$

As shown in Figure 7 (b), it can be calculated that the charge recombination time of DSCs without and with DCJTB coating are 10.01 ms

Table 1 | Photovoltaic parameters of DSCs with and without DCJTB coating

| Samples | $J_{sc}$/mA/cm$^2$ | $V_{oc}$/V | FF% | PCE/% |
|---|---|---|---|---|
| N3 | 12.96 | 0.650 | 50.4 | 4.27 |
| N3/DCJTB | 16.63 | 0.690 | 49.1 | 5.64 |

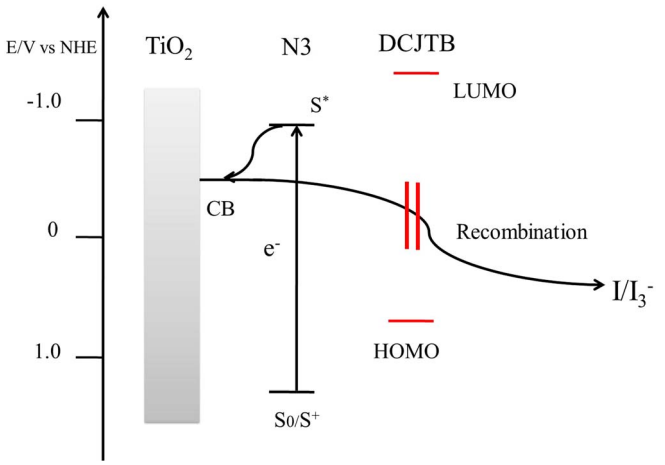


**Figure 6 | Diagrammatic drawing of retarding charge recombination of DSCs with DCJTB coating.**

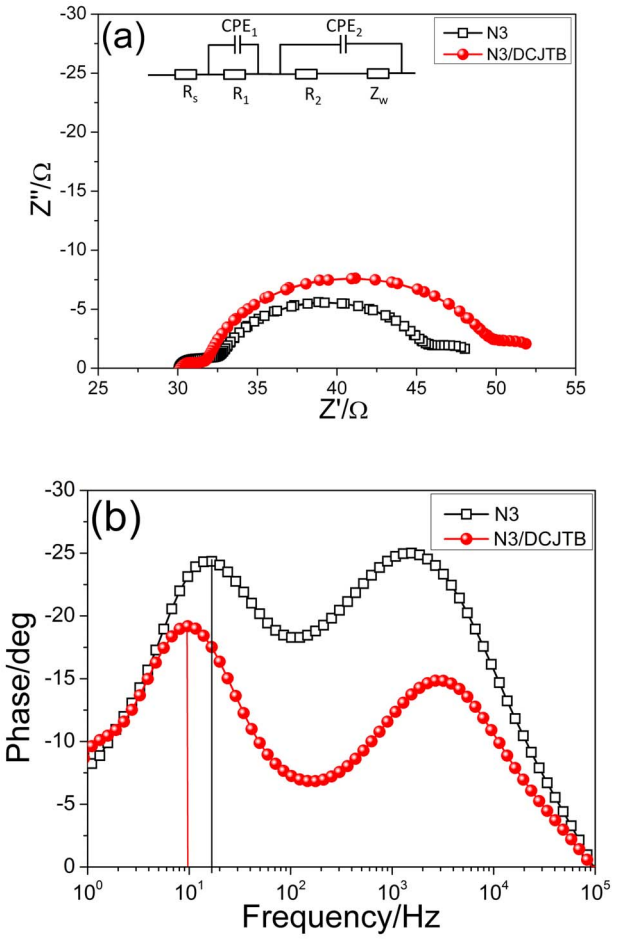


**Figure 7 | (a) Nyquist plots under dark condition (b) bode plots of DSCs with and without DCJTB coating.**

and 17.1 ms, respectively. As a result, it further indicates that DCJTB could retard the interface charge recombination in DSCs devices. The $V_{oc}$ of DSCs could be expressed by following equation[42–43]:

$$V_{oc} = \frac{RT}{\beta F} \ln\left(\frac{AI}{n_0 k_b [I_3^-] + n_0 k_r [D^+]}\right) \quad (4)$$

where $R$ is molar gas constant, $T$ is temperature in Kelvin, $F$ is Faraday constant, $\beta$ is the reaction order of $I_3^-$ and electrons, $A$ is the electrode area surface, $I$ is the incident photon flux, $n_0$ is the concentration of accessible electronic states in the conduction band. $k_b$ and $k_r$ are the kinetic constant of the back reaction and the recombination. $[I_3^-]$ and $[D^+]$ are concentrations of triiodide and oxidized dye, respectively. It could be considered that $f_{min}$ is as same as the back reaction constant ($k_b$)[44]. Thus from equation (4) it can be obtained that the longer charge recombination time causes the higher $V_{oc}$. It explains the increased $V_{oc}$ shown in Figure 5 (a) and Table 1.

To further explore the influence of the DCJTB interface modification on the electron diffusion and lifetime in DSCs under illumination, IMVS and IMPS spectra of DSCs with and without DCJTB coating have been tested. IMVS tests the same intensity perturbation but measures periodic modulation of the photovoltage giving the information of electron lifetime under open-circuit conditions at a given illumination intensity. Figure 8 (a) shows the results of IMVS test. It indicates that the electron lifetime has been increased when the DCJTB coating was introduced to the device, in a good agreement with retarding charge recombination as discussed earlier. IMPS measures the periodic photocurrent response to a small sinusoidal perturbation of the light intensity superimposed on a larger steady background level, which could provide information of the dynamics of charge transport and back reaction under short circuit conditions under certain illumination intensity[44].

$D_{eff}$ which represents the effective diffusion coefficient of electrons can be determined by the followed equation[45]

$$D_{eff} = D_0 \times \left(n_{free}/n_{total}\right) \quad (5)$$

where $n_{free}$ is the density of free electrons in the conduction band of $TiO_2$, and $n_{total}$ is the total density of free and trapped electrons.

As shown in Figure 8 (b), the electron diffusion coefficient of device with DCJTB coating clearly increases compared to that without DCJTB coating. It indicates that DCJTB coating is beneficial for electron transportation in DSCs. Such results also accord with the higher $J_{sc}$ in DSCs based on DCJTB coating, which is shown in Figure 5 (a) and Table 1. It could be due to the increased electron injection and decreased electron quenching and recombination, which increase the free electron in the photoanode. The increased electron injection is due to FRET between DCJTB and N3.

To weigh the electron transport and recombination properties, charge collection efficiency ($\eta_{coll}$) derived from IMPS and MVS measurements was apparently considered as meaningful parameter. In sensitized solar cells, $\eta_{coll}$ can be calculated by the followed equation[46]

$$\eta_{coll} = 1 - \tau_c/\tau_d \quad (6)$$

where $\tau_c$ is the electron collection time given by IMPS test and $\tau_d$ is the electron lifetime given by IMVS test. Figure 8(c) shows the charge collection efficiency of DCSs without and with DCJTB coating under different illumination intensity. It reveals that the charge collection efficiency increases with DCJTB coating, indicating it is beneficial to charge collection in photoanode of DSCs.

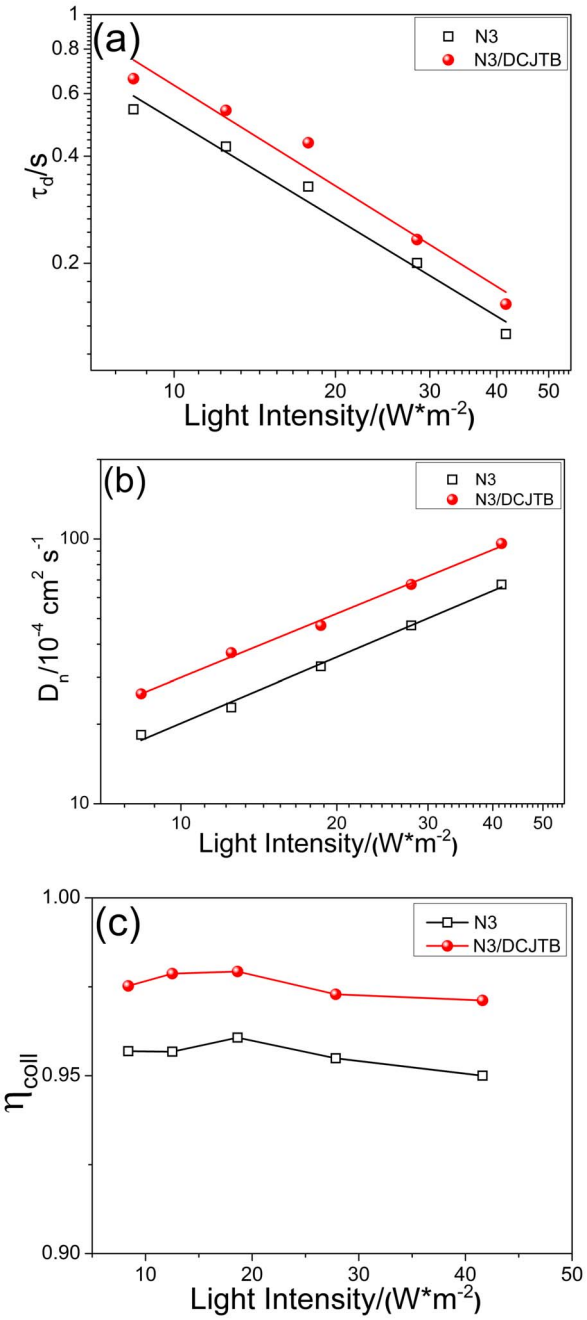


**Figure 8 | (a) IMVS (b) IMPS spectra and (c) electron collection efficiency of DSCs with and without DCJTB coating.**

## Conclusions

DCJTB as interface modification material has been used in DSCs, and it acts as a barrier layer retarding the charge recombination and resulted in increased photoresponse and electron injection efficiency due to the FRET at the interface of sensitized $TiO_2$ and electrolyte. Dip-coating method used in interface modification avoided electron quenching by concentrate ERD and acceptors on the surface of sensitized $TiO_2$. When DCJTB assembled on the surface of $TiO_2$, the distance between ERD and acceptors was reduced and thus, a higher FRET efficiency was achieved. With combining effects of retarding the charge recombination and FRET, DCJTB interface modification has significantly improved the photovoltaic performance of DSCs.

1. O' Regan, B. & Grätzel, M. A Low-cost, high-efficiency solar cell based on dye-sensitized colloidal $TiO_2$ films. *Nature* **353**, 737–740 (1991).
2. Tian, H. N., Yang, X. C., Chen, R. K., Hagfeldt, A. & Sun, L. C. A metal-free "black dye" for panchromatic dye-sensitized solar cells. *Energy Environ. Sci.* **2**, 674–677 (2009).
3. Burke, A., Schmidt-Mende, L., Ito, S. & Grätzel, M. A novel blue dye for near-IR 'dye-sensitised' solar cell applications. *Chem. Commun.* **3**, 234–236 (2007).

4. Enache-Pommer, E., Liu, B. & Aydil, E. S. Electron transport and recombination in dye-sensitized solar cells made from single-crystal rutile $TiO_2$ nanowires. *Phys. Chem. Chem. Phys.* **11**, 9648–9652 (2009).
5. Lan, Z. *et al.* Template-free synthesis of closed-microporous hybrid and its application in quasi-solid-state dye-sensitized solar cells. *Energy Environ. Sci.* **2**, 524–528 (2009).
6. Lee, K. M. *et al.* Highly porous PProDOT-Et-2 film as counter electrode for plastic dye-sensitized solar cells. *Phys. Chem. Chem. Phys.* **11**, 3375–3379 (2009).
7. Yella, A. *et al.* Porphyrin-sensitized solar cells with cobalt (II/III)-based redox electrolyte exceed 12 percent efficiency. *Science* **334**, 629–634 (2011).
8. Diamant, Y., Chen, S. G., Melamed, O. & Zaban, A. Core-shell nanoporous electrode for dye sensitized solar cells: the effect of the SrTiO3 shell on the electronic properties of the TiO2 core. *J. Phys. Chem. B* **107**, 1977–1981 (2003).
9. Bandaranayake, K. M. P., Senevirathna, M. K. I., Weligamuwa, P. & Tennakone, K. Dye-sensitized solar cells made from nanocrystalline TiO2 films coated with outer layers of different oxide materials. *Coord. Chem. Rev* **248**, 1277–1281 (2004).
10. Liu, Z. Y. *et al.* $Al_2O_3$-coated $SnO_2/TiO_2$ composite electrode for the dye-sensitized solar cell. *Electrochimica Acta* **50**, 2583–2589 (2005).
11. Chen, S. G., Chappel, S., Diamant, Y. & Zaban, A. Preparation of $Nb_2O_5$ coated $TiO_2$ nanoporous electrodes and their application in dye-sensitized solar cells. *Chem. Mater* **13**, 4629–4634 (2001).
12. Palomares, E., Clifford, J. N., Haque, S. A., Lutz, T. & Durrant, J. R. Control of charge recombination dynamics in dye sensitized solar cells by the use of conformally deposited metal oxide blocking layers. *J. Am. Chem. Soc* **125**, 475–482 (2003).
13. Gao, R., Wang, L. D., Ma, B. B., Zhan, C. & Qiu, Y. $Mg(OOCCH_3)_2$ Interface Modification after Sensitization to Improve Performance in Quasi-solid Dye-Sensitized Solar Cells. *Langmuir* **26**, 2460–2465 (2010).
14. Luo, F., Wang, L. D., Ma, B. B. & Qiu, Y. Post-modification using aluminum isopropoxide after dye-sensitization for improved performance and stability of quasi-solid-state solar cells. *J. Photochem. Photobio. A: Chem* **197**, 375–381 (2008).
15. Fischer, A. *et al.* Crystal formation involving 1-methylbenzimidazole in iodide/triiodide electrolytes for dye-sensitized solar cells. *Sol. Energy Mater. Sol. Cells* **91**, 1062–1065 (2007).
16. Gao, R. *et al.* Interface modification of 8-hydroxyquinoline aluminium with combined effects in quasi-solid dye-sensitized solar cells. *Phys. Chem. Chem. Phys.* **14**, 5973–5978 (2012).
17. Forster, T. 10th spiers memorial lecture-transfer mechanism of electronic excitation. *Discuss. Faraday Soc.* **27**, 7–17 (1959).
18. Algar, W. *et al.* Emerging non-traditional Förster resonance energy transfer configurations with semiconductor quantum dots: Investigations and applications. *Coordin. Chem. Rev.* **263–264**, 65–85 (2014).
19. Lee, E., Kim, C. & Jang, J. High-performance Foerster resonance energy transfer (FRET)-based dye-sensitized solar cells: rational design of quantum dots for wide solar-spectrum utilization. *Chem.-Eur. J.* **19**, 10280–10286 (2013).
20. Sarkar, S. *et al.* Dual-Sensitization via Electron and Energy Harvesting in CdTe Quantum Dots Decorated ZnO Nanorod-Based Dye-Sensitized Solar Cells. *J. Phys. Chem. C.* **116**, 14248–14256 (2012).
21. Cheon, J. H. *et al.* Enhancement of light harvesting in dye-sensitized solar cells by using Foerst-type resonance energy transfer. *Met. Mater. Int.* **19**, 1365–1368 (2013).
22. Cheon, J. H. *et al.* Enhanced light-harvesting efficiency by Forster resonance energy transfer in quasi-solid state DSSC using organic blue dye. *Electrochim. Acta.* **68**, 240–245 (2012).
23. Basham, J. I. *et al.* Forster Resonance Energy in Dye-Sensitized Solar Cells. *ACS Nano.* **4**, 1253–1258 (2010).
24. Hardin, B. E. *et al.* High Excitation Transfer Efficiency from Energy Relay Dyes in Dye-Sensitized Solar Cells. *Nano. Lett.* **10**, 3077–3083 (2010).
25. Gao, R. *et al.* Effects of an Intercalation Nanocomposite at the Photoanode/Electrolyte Interface in Quasi-Solid Dye-Sensitized Solar Cells. *J. Phys. Chem. C* **115**, 17986–17992 (2011).
26. Gao, R. *et al.* Interface modification effects of 4-tertbutylpyridine interacting with N3 molecules in quasi-solid dye-sensitized solar cells. *Phys. Chem. Chem. Phys.* **13**, 10635–10640 (2011).
27. Shi, J. M. & Tang, C. W. Doped organic electroluminescent devices with improved stability. *Appl. Phys. Lett.* **70**, 1665–1667 (1997).
28. Shklover, V., Ovchinnikov, Y. E., Braginsky, L. S., Zakeeruddin, S. M. & Grätzel, M. Structure of Organic/Inorganic Interface in Assembled Materials Comprising Molecular Components. Crystal Structure of the Sensitizer Bis[(4,4′-carboxy-2,2′-bipyridine)(thiocyanato)] ruthenium(II). *Chem. Mater.* **10**, 2533–2541 (1998).
29. Chen, C. H., Tang, C. W., Shi, J. & Klubek, K. P. Improved red dopants for organic electroluminescent devices. *Macromolecular Symposia* **125**, 49–58 (1998).
30. Shi, Y. T. *et al.* The electrically conductive function of high-molecular weight poly(ethylene oxide) in polymer gel electrolytes used for dye-sensitized solar cells. *Phys. Chem. Chem. Phys.* **11**, 4230–4235 (2009).
31. Hong, Y., Jacky, W., Lam, Y. & Tang, B. Z. Aggregation-induced emission: phenomenon, mechanism and applications. *Chem. Commun.* 4332–4353 (2009).
32. Yum, J. H. *et al.* Incorporating multiple energy relay dyes in liquid dye-sensitized solar cells. *ChemPhysChem.* **12**, 657–661 (2011).
33. Yum, J. H. *et al.* Panchromatic Response in Solid-State Dye-Sensitized Solar Cells Containing Phosphorescent Energy Relay Dyes. *Angew. Chem. Int. Ed.* **48**, 9277–9280 (2009).
34. Hardin, B. E. *et al.* Increased light harvesting in dye-sensitized solar cells with energy relay dyes. *Nat. Photonics.* **3**, 406–411 (2009).
35. Tang, C. W. & Vanslyke, S. A. Organic electroluminescent diodes. *Appl. Phys. Lett.* **51**, 913–915 (1987).
36. Grätzel, M. Photoelectrochemical cells. *Nature* **414**, 338–344 (2001).
37. Wang, Q., Moser, J. E. & Gratzel, M. Electrochemical impedance spectroscopic analysis of dye-sensitized solar cells. *J. Phys. Chem. B* **109**, 14945–14953 (2005).
38. Qin, D. *et al.* Ionic liquid/polymer composite electrolytes by in situ photopolymerization and their application in dye-sensitized solar cells. *Electrochim. Acta* **56**, 8680–8687 (2011).
39. Gao, R. *et al.* Photovoltaic Properties and Mechanism Analysis of a Dye/$Al_2O_3$ Alternating Assembly Structure by Electrochemical Impedance Spectroscopy. *Acta. Phys-Chim. Sin.* **27**, 413–418 (2011).
40. Gao, R., Niu, G. D., Wang, L. D., Ma, B. B. & Qiu, Y. N3/$Al_2O_3$/N749Alternating Assembly Structure Broadening the Photoresponse and Interface Modification Effects in Quasi-Solid Dye-Sensitized Solar Cells. *Acta. Phys-Chim. Sin.* **29**, 73–81 (2013).
41. Kern, R., Sastrawan, R., Ferber, J., Stangl, R. & Luther, J. Modeling and interpretation of electrical impedance spectra of dye solar cells operated under open-circuit conditions. *Electrochim. Acta* **47**, 4213–4225 (2002).
42. Lee, K., Park, S. W., Ko, M. J., Kim, K. & Park, N. G. Selective positioning of organic dyes in a mesoporous inorganic oxide film. *Nat. Mater* **8**, 665–671 (2009).
43. Adachi, M., Sakamoto, M., Jiu, J., Ogata, Y. & Isoda, S. Determination of parameters of electron transport in dye-sensitized solar cells using electrochemical impedance spectroscopy. *J. Phys. Chem. B* **110**, 13872–13880 (2006).
44. Bisquert, J. Theory of the Impedance of Electron Diffusion and Recombination in a Thin Layer. *J. Phys. Chem. B* **106**, 325–333 (2002).
45. Dloczik, L. *et al.* Dynamic Response of Dye-Sensitized Nanocrystalline Solar Cells: Characterization by Intensity-Modulated Photocurrent Spectroscopy. *J. Phys. Chem. B* **101**, 10281–10289 (1997).
46. Hagfeldt, A., Boschloo, G., Sun, L. C., Kloo, L. & Pettersson, H. Chem. Dye-Sensitized Solar Cells. *Chem. Rev.* **110**, 6595–6663 (2010).


## Acknowledgments

This work was supported by the National Natural Science Foundation of China under Grant No. 51273104 and the National Key Basic Research and Development Program of China under Grant No. 2009CB930602.

## Author contributions

L.W. proposed the conceptual idea and provided financial support through grant application. G.R. participated in the analysis of results, discussing and writing the manuscript. Y.C. and X.L. participated in discussing the results and in writing the manuscript. All authors read and approved the final manuscript.

## Additional information

**Competing financial interests**: The authors declare no competing financial interests.

**How to cite this article:** Gao, R., Cui, Y.X., Liu, X.J. & Wang, L.D. Multifunctional Interface Modification of Energy Relay Dye in Quasi-solid Dye-sensitized Solar Cells. *Sci. Rep.* **4**, 5570; DOI:10.1038/srep05570 (2014).